

X-RAY PHOTOELECTRON SPECTROSCOPY INVESTIGATION OF NITROGEN TRANSFORMATION IN CHINESE OIL SHALES DURING PYROLYSIS

QING WANG^{*}, QI LIU, ZHICHAO WANG,
HONGPENG LIU, JINGRU BAI

Engineering Research Centre of Oil Shale Comprehensive Utilization, Ministry of Education, Northeast Electric Power University, Jilin, Jilin 132012, People's Republic of China

Abstract. X-ray photoelectron spectroscopy (XPS) was used to investigate changes in nitrogen functionalities present in Chinese Huadian (HD), Maoming (MM) and Yaojie (YJ) oil shales during pyrolysis. Throughout the process ($T \leq 600$ °C), most of the nitrogen contained in raw oil shale samples was retained in their semi-cokes. Five peaks of nitrogen functionalities (N 1s) appeared in the XPS spectra of raw HD, MM and YJ oil shale samples and their semi-cokes: N-6 (pyridine), N-A (amino), N-5 (pyridone), N-Q (quaternary nitrogen) and N-X1 (pyridine N-oxide). To obtain an acceptable fit, an additional peak at $404 (\pm 0.5)$ eV (N-X2) was required in the N 1s spectra of the samples. N-5 could either represent pyridone or a mixture of pyridone and pyrrolic nitrogen forms, the most abundant ones in all samples. At a relatively low temperature (300 °C) the desorption reaction occurred and the amount of chemisorbed oxygen associated nitrogen (N-X2) decreased significantly. As the pyrolysis temperature increased from 300 to 500 °C, pyridine N-oxide was converted to pyridone, and, simultaneously, the latter was converted to pyridine and pyridine structures associated with oxygen – quaternary nitrogen. In the semi-cokes of Huadian and Maoming oil shale samples at 600 °C, most of the pyridone was converted into pyridine and quaternary nitrogen. At this temperature, especially the condensation reaction of pyridine into quaternary nitrogen occurred in the semi-coke of Yaojie oil shale sample, while quaternary nitrogen represented the nitrogen atoms in the interior of precursors of the graphene layers.

Keywords: oil shale pyrolysis, semi-coke, nitrogen transformation, X-ray photoelectron spectroscopy.

^{*} Corresponding author: e-mail rlx888@126.com

1. Introduction

Oil shale is a sedimentary rock that consists of the mineral and organic parts [1], the latter being primarily composed of kerogen. As an unconventional oil and gas resource, oil shale is a very important kind of alternative energy in the 21st century, due to its rich natural resources, favorable characteristics, and feasibility of utilization [2]. At present, oil shale is mainly pyrolyzed to yield shale oil and is burnt directly as a fuel to generate electricity [3]. Nitrogen-containing functional groups present in oil shale can be transformed into various compounds and are distributed in semi-coke, shale oil and gases during pyrolysis. But one has to consider that these nitrogen compounds impair the quality of shale oil products and also seriously pollute the environment [4–8]. In order to understand the mechanism of formation of these nitrogen-containing pollutants, it is important to determine the fate of nitrogen functionalities during the pyrolysis of oil shale. This help to find ways to improve the quality of shale oil products, to protect the environment and also to contribute to a more rational utilization of oil shale resources. Moreover, despite the fact that nitrogen is present in oil shale in lower amounts compared with carbon and hydrogen, it is associated with carbon atoms in various structural forms, which are the key components in the entire molecular structure of oil shale. Hence, to have a better understanding of the chemical structure of oil shale, it is necessary to investigate the nitrogen structural forms and their distribution in it.

X-ray photoelectron spectroscopy (XPS) [9–13] and X-ray absorption near edge spectroscopy (XANES) [14–16] showed that pyrrolic and pyridine forms were the major nitrogen functionalities present in raw coals. In addition, quaternary, amino and oxidized nitrogen functionalities were also found. XPS was employed to study the fate of nitrogen functionalities during the pyrolysis of coal or model compounds as well. Kelemen et al. [10, 17] found that the amount of quaternary nitrogen decreased during the mild pyrolysis (400 °C) of coals and increased in severe conditions of the process. The investigators proposed that the decrease in the amount of quaternary nitrogen was associated with the loss of nearby or adjacent hydroxyl groups from carboxylic acids or phenols. The increase in the quaternary nitrogen content was attributed to the incorporation of nitrogen into large polynuclear aromatic carbon structures. Amino groups were released first and concentrated in tar, during the pyrolysis of low-rank coal [17]. Stańczyk et al. [18] observed that a relatively low pyrolysis temperature made nitrogen functionalities transform into the structures with higher thermal stability during the pyrolysis of the model compound. Also, mutual transformations could occur between pyridine and pyrrolic groups. Pels et al. [19] found that pyridones, protonated pyridine and N-oxides of pyridine groups were converted to pyridine nitrogen during the mild pyrolysis of lignite. With pyrolysis conditions becoming more severe, all forms of nitrogen were eventually present in 6-membered rings. Nitrogen located at the edges of the graphene

layers was pyridine nitrogen and the one located in the interior of the layers was quaternary nitrogen. A lot of information about the nitrogen functionalities in coal has been obtained by XPS so far. At the same time, very little or no information is available on the thermal transformation of these functionalities during oil shale pyrolysis. Considering this, in the current paper, the distribution of nitrogen functionalities in different Chinese oil shales and their semi-cokes obtained at various pyrolysis temperatures has been investigated.

2. Experimental

2.1. Sample preparation

Three typical, relatively high-nitrogen Chinese oil shales – Huadian (HD), Maoming (MM), and Yaojie (YJ), were chosen for the present study. The organic matter (OM) of HD oil shale belongs to type I kerogen, that of YJ oil shale is type II kerogen, whereas the OM of MM oil shale appears to be between type I and type II kerogens [20]. The results of proximate and ultimate analyses of raw oil shale samples are presented in Table 1. As seen from the table, all three oil shale samples have a low content of fixed carbon (FC) and a high content of ash (A). However, in the HD oil shale sample, the proportion of ash is lower but oil content higher than in the other two samples. The semi-cokes of three oil shales were obtained in the Fischer Assay device, which consisted of an aluminum retort and an electric furnace with temperature program function [21]. An aluminum retort containing 50 (± 0.5) g of oil shale was placed in an electric furnace. Then the reactor was heated at a heating rate of 5 °C/min from room temperature to 300 °C, after a soak time of 30 s. After that the retort was removed from the electric furnace and cooled to room temperature, avoiding contact with air. A similar procedure was also followed to obtain semi-cokes by heating the reactor from room temperature to 400, 500 and 600 °C. The raw oil shale samples and the obtained semi-cokes were ground to < 200 mesh and stored in a vacuum dryer for XPS analyses.

Table 1. Proximate and ultimate analyses of raw oil shale samples

Sample	Proximate analysis, $w_{ad}\%$				Ultimate analysis, $w_{ad}\%$					Oil ^b
	M	A	V	FC	C	H	N	O ^a	S _t	
HD	3.81	55.54	36.61	4.04	29.36	4.55	0.54	5.39	0.81	12.45
MM	2.33	70.61	20.87	6.19	15.97	2.65	0.66	6.42	1.36	8.82
YJ	1.10	69.32	25.21	4.37	18.32	2.79	0.45	6.80	1.22	7.15

Note: M – moisture; A – ash; V – volatile; FC – fixed carbon; _{ad} – air-dried basis; ^a – oxygen by difference; S_t – total sulfur; ^b – percentage by Fischer Assay. Abbreviations used: HD – Huadian, MM – Maoming, YJ – Yaojie.

2.2. X-ray photoelectron spectroscopy

The X-ray photoelectron spectroscopy analysis of raw oil shale samples and the obtained semi-cokes was performed on a Thermo VG Scientific ESCALAB 250 Xi spectrometer, which was equipped with a microfocusing monochromator and a charge compensation system. The monochromatic Al K α (1486.6 eV) X-ray source was operated at 150 W in the constant analyzer energy mode and used with a spot size of 500 μm in diameter. While recording the spectra of the samples, all corrections to binding energies arising from charging were made assigning a binding energy of 284.8 eV to the principal C 1s component. The pass energies of the survey and narrow spectra were fixed at 100 and 30 eV, respectively. In order to obtain a good experimental effect, the powdered oil shale samples were compressed into tablets by a tablet press for XPS analysis.

Some studies [10, 22–24] investigated the curve-resolved method of XPS N 1s spectra and reported the forms of organic nitrogen in coals and oil shale kerogens. These forms included pyridine, amino, pyrrolic and quaternary nitrogen functionalities, which corresponded to fit peaks at 398.6, 399.4, 400.2 and 401.4 (± 0.1) eV, designated as N-6, N-A, N-5 and N-Q, respectively. A schematic picture of the nitrogen functionalities in HD, MM and YJ oil shales is shown in Figure 1. It should be noted that the binding energy of pyridone is close to that of pyrrolic nitrogen, and hence they cannot be distinguished by XPS. The exact nature of the quaternary nitrogen functionality could not be well established and it was probably present in the form of protonated pyridine nitrogen or in other forms [17]. When the N 1s spectra of raw oil shale samples and semi-cokes were curve-resolved, it was necessary to obtain a satisfactory fit for the peaks at 403 (± 0.5) and 404 (± 0.5) eV. The two peaks were referred to as N-X1 and N-X2, respectively. It was difficult to define the nature of the components of N-X1 and N-X2. Pietrzak and Wachowska [23] reported that the curve-resolved peak at the binding energy of 402.8 eV was attributed to pyridine N-oxide and peaks in the region of 402–406 eV were assigned to oxygen chemisorbed onto nitrogen in the XPS N 1s spectra of coals. Kelemen et al.

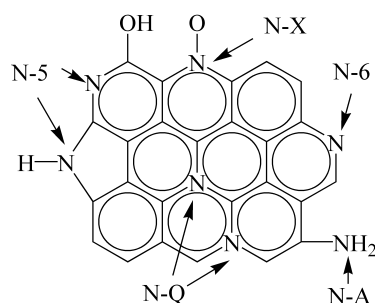


Fig. 1. Schematic representation of the nitrogen functionalities in Huadian, Maoming and Yaojie oil shales.

[10] inferred that the curve-resolved peak at around 403 eV was due to pyridine N-oxide in coals. In all cases the N 1s spectra were curve-resolved using the full width at half maximum (fwhm) of 1.4 (± 0.1) eV and a mixed 70% Gaussian 30% Lorentzian line shape. The Shirley-type background was subtracted prior to peak fitting. The peak shape and peak energy positions were fixed in the curve resolution process and only the amplitudes of these peaks were varied to obtain the best fit with the XPS N 1s spectra. Since the relative sensitivity factors for X-ray photoelectron spectroscopy of the same element under different chemical states are equal, the relative percentage of each area of the curve-resolved peak is equal to the relative mole percentage of nitrogen in its chemical state.

3. Results and discussion

3.1. Changes in nitrogen contents during pyrolysis

3.1.1. Ultimate analysis

The ultimate analysis of the semi-cokes of Chinese oil shale samples obtained at different temperatures was carried out, and the rates of nitrogen removal were calculated based on these analytical data. The results are presented in Table 2. The rates of nitrogen removal were calculated using the following formula [25]:

$$\eta = \frac{W_0 N_0 - W_0 N_1 \omega}{W_0 N_0} \times 100\%,$$

where η is the rate of nitrogen removal, W_0 is the mass of raw oil shale sample, N_0 is the nitrogen content of raw oil shale sample, N_1 is the nitrogen content of semi-cokes obtained at different temperatures, ω is the yield of semi-coke, i.e. the ratio of the mass of semi-coke sample to the mass of raw oil shale sample (on air-dried basis in all cases).

As seen from Table 2, with increasing pyrolysis temperature the yield of the semi-coke of HD, MM, and YJ oil shale samples decreases. There is a decline of more than 9% in the temperature range of 400–500 °C. The reason is that in this temperature region most of the shale oil is generated [26–28], which results in the decrease of semi-coke yield. It is especially interesting to note that the mass losses of all three oil shale samples during pyrolysis from room temperature to 300 °C approximately correspond to their water contents given in Table 1. This suggests that the removal of water from the samples is the most significant process in this pyrolysis temperature range. The rate of removal of nitrogen increases with increase in pyrolysis temperature, the highest increases occurring in the 400–500 °C temperature region. In this temperature range, the rate of nitrogen removal in case of HD oil shale sample increases by 34.45%, as against respectively 22.47 and 20.59% in case of MM and YJ oil shale samples. When the pyrolysis tem-

Table 2. Ultimate analysis of and nitrogen removal from semi-cokes obtained at different temperatures

Oil shale	Sample	Content, $w_{ad}\%$			Semi-coke yield ω , %	Nitrogen removal η , %
		C	H	N		
HD	300 °C semi-coke	29.83	4.47	0.55	96.48	1.73
	400 °C semi-coke	29.48	4.26	0.56	92.72	3.84
	500 °C semi-coke	13.55	1.46	0.48	69.42	38.29
	600 °C semi-coke	11.36	0.96	0.43	66.20	47.28
MM	300 °C semi-coke	16.26	2.56	0.67	97.37	1.16
	400 °C semi-coke	15.37	2.25	0.67	95.77	2.78
	500 °C semi-coke	9.39	1.18	0.57	86.56	25.25
	600 °C semi-coke	8.78	0.63	0.53	82.79	33.01
YJ	300 °C semi-coke	18.64	2.71	0.45	98.62	1.38
	400 °C semi-coke	18.49	2.57	0.45	97.78	2.22
	500 °C semi-coke	10.98	1.37	0.40	86.84	22.81
	600 °C semi-coke	9.87	0.96	0.38	80.46	32.06

Note: a_d – air-dried basis. Abbreviations used: HD – Huadian, MM – Maoming, YJ – Yaojie.

perature reaches 600 °C, the rate of nitrogen removal is the highest in case of HD oil shale sample, followed by MM and YJ oil shale samples. This corresponds to the decreasing oil contents of the samples as measured by the Fischer Assay method (Table 1). In summary, most of the nitrogen present in three raw oil shale samples is retained in their semi-cokes. In addition, the rate of nitrogen removal is directly proportional to the shale oil content of the samples.

3.1.2. X-ray photoelectron spectroscopy analysis

The nitrogen contents of raw oil shale samples and the semi-cokes obtained at different temperatures were analyzed by XPS, the analysis results are presented in Table 3. From the table it can be seen that in raw oil shale samples and the obtained semi-cokes the relative amounts of oxygen are higher than those of carbon and nitrogen. This is due to that oxygen in the analyzed samples exists in both the organic form and the inorganic form. The proximate analysis of raw oil shale samples indicates that their ash (A) contents are higher than 55%, while that of MM oil shale sample amounts to even 70.61% (Table 1). Some studies [29, 30] found that minerals in oil shales existed as kaolinite, hydromica, quartz, etc. The high content of inorganic oxygen in these minerals enhances the intensity of the oxygen signal in XPS analysis, which is indicative of oxygen abundance in the oil shales studied. When the pyrolysis temperature increases from room temperature to 400 °C, the number of nitrogen atoms per 100 carbon atoms (the nitrogen-to-carbon ratio) in the oil shale samples under study decreases constantly. It is not yet clear whether the rate of release of nitrogen atoms is

Table 3. XPS analysis of raw oil shale samples and semi-cokes obtained at different temperatures

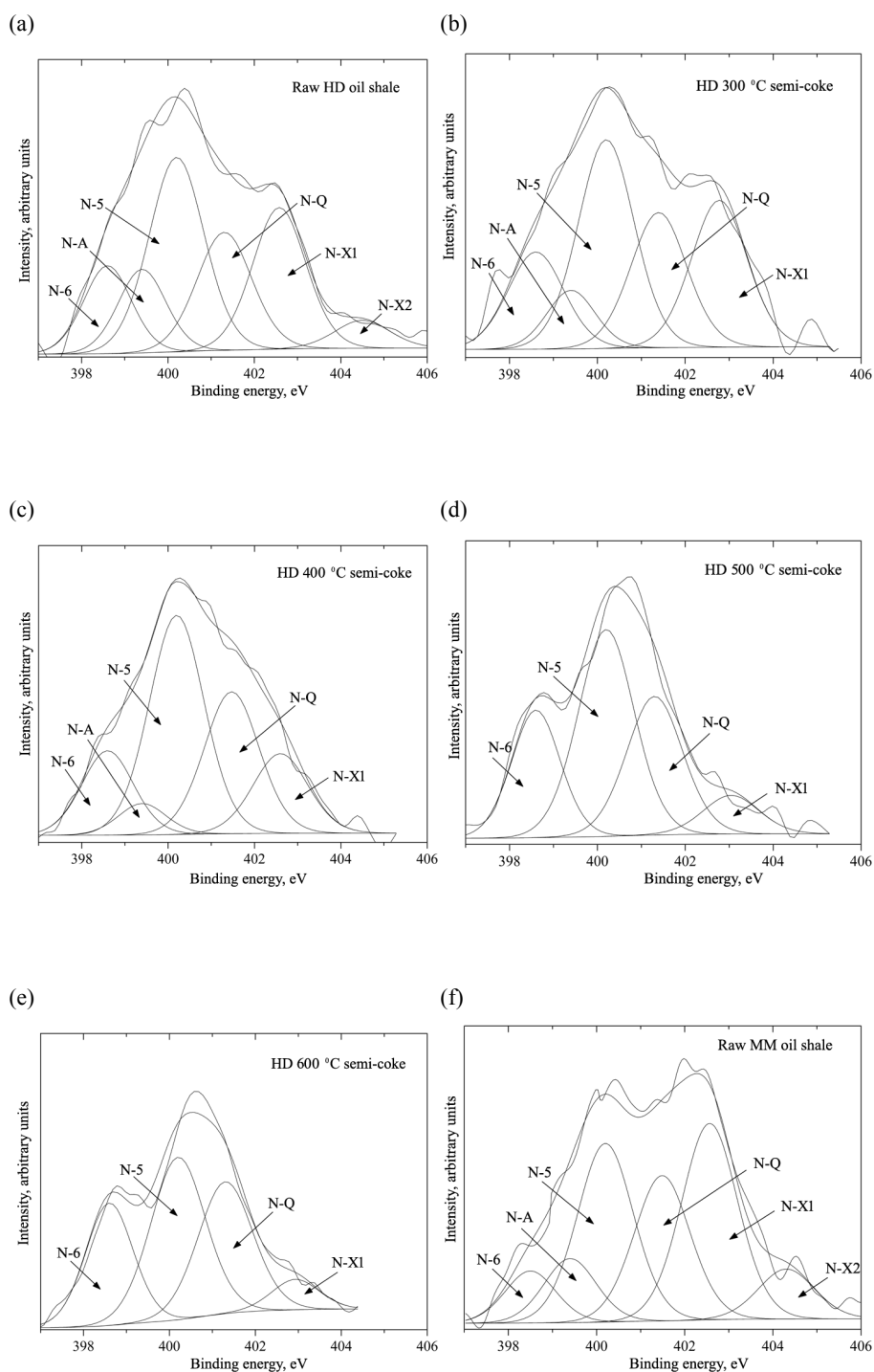
Oil shale	Sample	Carbon, mol%	Oxygen, mol%	Nitrogen, mol%	Nitrogen atoms per 100 carbon atoms
HD	Raw oil shale	41.2	57.7	1.1	2.6
	300 °C semi-coke	42.4	56.7	1.0	2.4
	400 °C semi-coke	49.2	49.9	0.9	1.9
	500 °C semi-coke	45.5	53.4	1.1	2.3
	600 °C semi-coke	36.3	62.6	1.1	3.1
MM	Raw oil shale	28.3	70.4	1.3	4.6
	300 °C semi-coke	32.2	66.4	1.4	4.3
	400 °C semi-coke	44.7	53.6	1.7	3.7
	500 °C semi-coke	42.8	55.4	1.8	4.1
	600 °C semi-coke	42.6	55.9	1.5	3.6
YJ	Raw oil shale	32.8	66.2	1.0	3.0
	300 °C semi-coke	33.7	65.4	0.9	2.7
	400 °C semi-coke	38.6	60.4	1.0	2.6
	500 °C semi-coke	43.4	54.8	1.8	4.1
	600 °C semi-coke	41.4	57.2	1.4	3.3

Abbreviations used: HD – Huadian, MM – Maoming, YJ – Yaojie.

higher than that of carbon atoms or their rate of enrichment is lower than that of carbon atoms. However, the nitrogen-to-carbon ratio increases when the pyrolysis temperature increases to 500 °C. Since a high quantity of volatile hydrocarbons is generated and released into the gaseous phase in the temperate range of 400–500 °C, the rate of release of nitrogen atoms is lower than that of carbon atoms in this temperature region. As the pyrolysis temperature is further increased to 600 °C, the nitrogen-to-carbon ratio in MM and YJ oil shale samples decreases significantly, while in the case of HD oil shale sample, the increase is continuous. This may be explained by that the release of volatile hydrocarbons from MM and YJ oil shale samples tends to end and the rate of release of carbon atoms drops sharply. However, the amounts of nitrogen atoms in MM and YJ oil shale samples decrease at 600 °C, which indicates that their rate of release is continuously high. Nevertheless, the oil content of HD oil shale sample is much higher than those of the other two samples, so the release of carbon atoms from it is not over by 600 °C. As a result, the nitrogen-to-carbon ratio of HD oil shale sample still increases.

3.2. Evolution of nitrogen functionalities during pyrolysis

Figures 2 and 3 show the XPS N 1s spectra of raw HD, MM, and YJ oil shale samples and their semi-cokes obtained at different pyrolysis temperatures. These spectra are fitted by five peaks: 398.6 eV (N-6), 399.4 eV (N-A), 400.2 eV (N-5), 401.4 (± 0.1) eV (N-Q), and 403 (± 0.5) eV (N-X1). To obtain an acceptable fit, an additional peak at 404 (± 0.5) eV (N-X2) is



(to be continued)

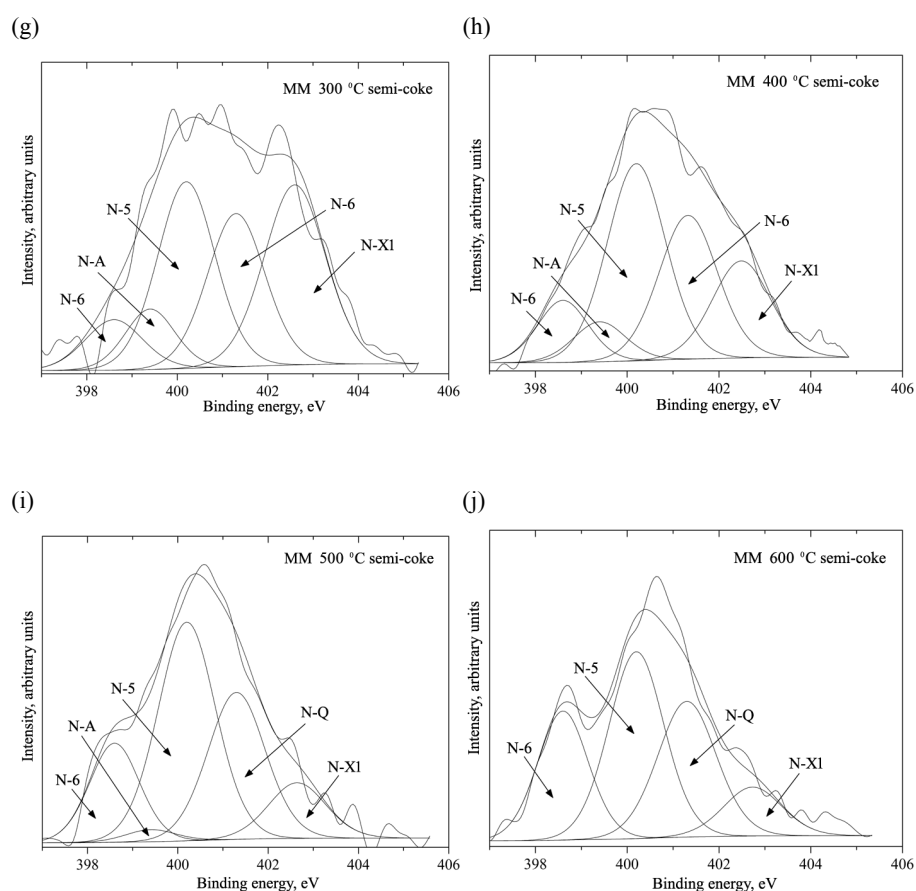


Fig. 2. XPS N 1s spectra of raw Huadian and Maoming oil shale samples and their semi-cokes obtained at different temperatures. Included in the figure are the curve resolution results. Abbreviations used: HD – Huadian, MM – Maoming.

required in the N 1s spectra of raw oil shale samples. In all spectra, the peak at 400.2 eV (N-5) is the highest one, which implies that in all samples the relative amounts of pyridone are the highest throughout pyrolysis, except for the raw MM oil shale sample and its semi-coke obtained at 300 °C. In the latter cases, the relative amounts of pyridine N-oxide are the highest, whereas those of pyridone are somewhat lower. Nitrogen functionalities present in all three raw oil shale samples are the same and appear in six forms. Some previous studies [10, 11, 17, 19] reported only four species of nitrogen functionalities in raw coals. In contrast to these coals, nitrogen in the studied raw oil shale samples appears in more numerous chemical states, which are complex in nature.

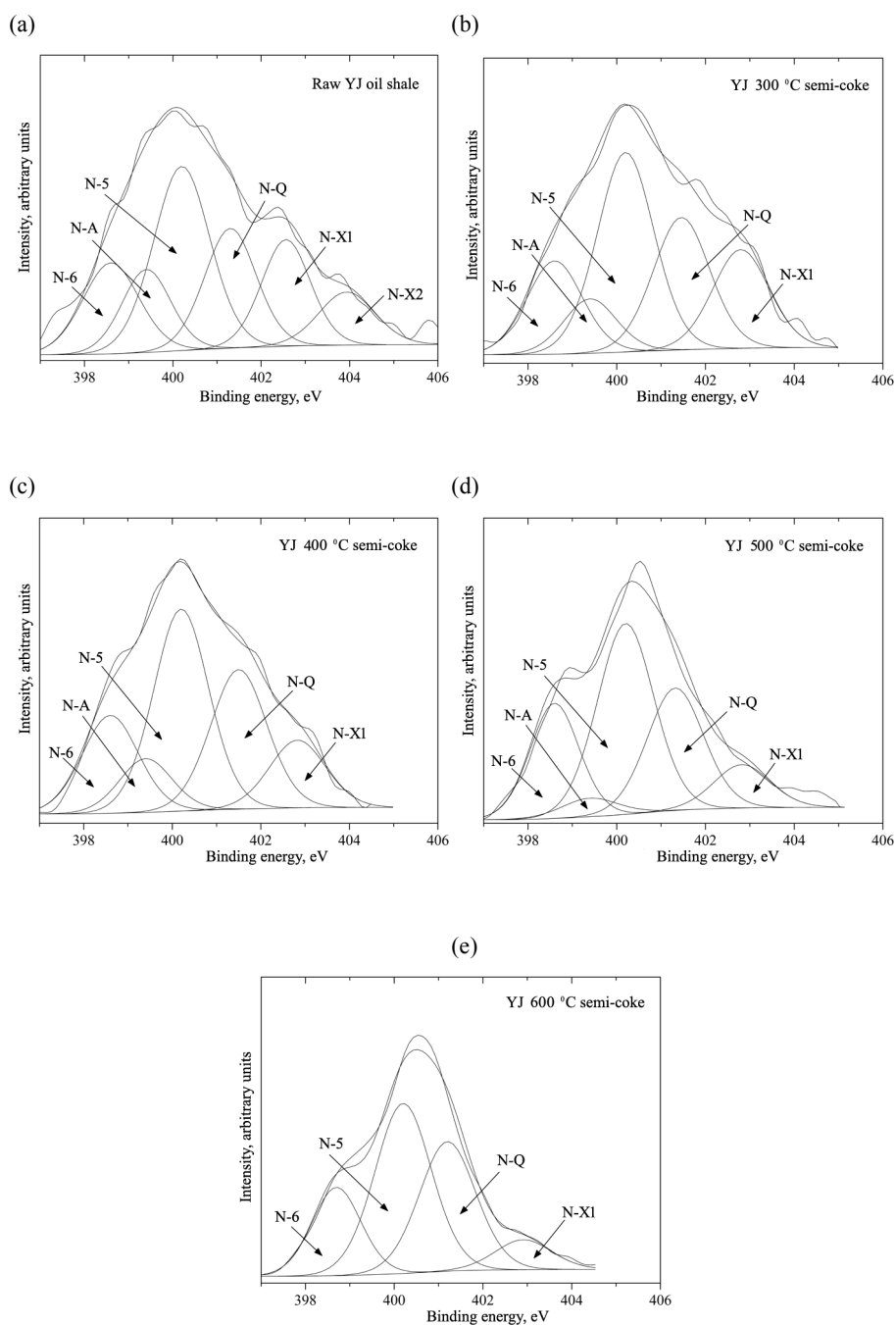


Fig. 3. XPS N 1s spectra of raw Yaojie oil shale sample and its semi-coke obtained at different temperatures. Included in the figure are the curve resolution results. Abbreviation used: YJ – Yaojie.

The relative amounts of nitrogen functionalities present in raw oil shale samples and the semi-cokes obtained at different pyrolysis temperatures are found from the curve resolutions of N 1s spectra. Figure 4 shows the relative amounts of nitrogen functionalities as a function of temperature during the pyrolysis of HD, MM and YJ oil shale samples. Significant changes in the distribution of these functionalities occur during the process. As seen from Figure 4f, when the pyrolysis temperature reaches 300 °C, the relative amount of oxygen chemisorbed nitrogen decreases significantly. The peak at 404(±0.5) eV (N-X2) disappears in the fitting results in the spectra of semi-cokes (Figs. 2 and 3), which indicates that the relative amount of the compound is below the detection limit of XPS. It is likely that these components in the binding energy region of 402–406 eV arise due to the oxygen chemisorbed nitrogen on the sample surface [23, 31]. The nitrogen form present on the surfaces of raw oil shale samples is probably due to that the samples had remained in an open environment for a long time. When raw oil shale samples are heated to 300 °C, the desorption reaction occurs due to the low thermal stability of the oxygen chemisorbed onto nitrogen. Hence, the relative amount of N-X2 nitrogen decreases dramatically.

The relative amount of amino nitrogen decreases gradually with increasing pyrolysis temperature, as shown in Figure 4b. The curve-resolved peaks that correspond to amino nitrogen disappear from the spectrum of the semi-coke of HD oil shale sample at 500 °C and from the spectra of semi-cokes of MM and YJ oil shale samples at 600 °C. Kelemen et al. [17] reported that in the case of low-rank coal, mainly amino nitrogen was released and concentrated in tar. Stańczyk et al. [18] concluded that the amino nitrogen present in 9-aminoacridine and 3-aminoanthracene had a low thermal stability and the corresponding peaks disappeared from the spectra of chars on pyrolysis at 460 °C. In the current study, the amino nitrogen present in three oil shale samples is mainly released into the gaseous phase. It is interesting to note that the relative amount of amino nitrogen in the HD oil shale sample drops significantly faster than those in MM and YJ oil shale samples, during pyrolysis. This indicates that the thermal stability of amino nitrogen in the HD oil shale sample is lower. This may be explained by that amino nitrogen can be either in the aliphatic form or in the aromatic form. The thermal stability of aliphatic amino is lower than that of aromatic amino. Hence, the proportion of the former in the HD oil shale sample is higher than in MM and YJ oil shale samples.

It can be observed in Figure 4e that the relative amounts of quaternary nitrogen increase continuously with increasing pyrolysis temperature. This shows that the quaternary nitrogen present in three oil shale samples has a high thermal stability. Pels et al. [19] found that the nature of quaternary nitrogen could not be defined, based on model compounds, and claimed that in lignite it could correspond to the protonated pyridine nitrogen. Kelemen et al. [22] suggested that there might be other forms of quaternary nitrogen, in

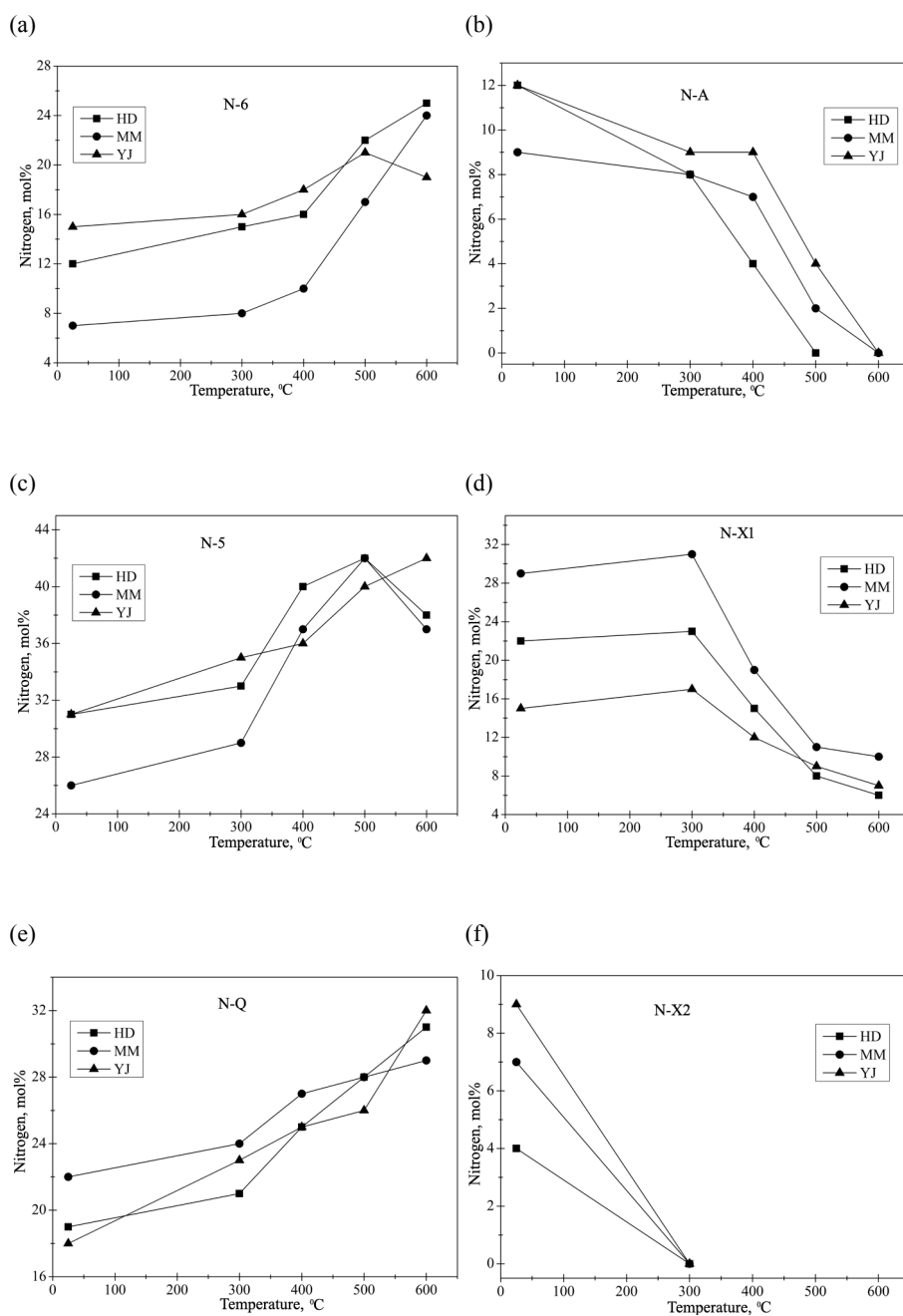


Fig. 4. The relative amounts of nitrogen functionalities as a function of temperature during pyrolysis of Huadian, Maoming and Yaojie oil shale samples. Abbreviations used: HD – Huadian, MM – Maoming, YJ – Yaojie.

addition to the protonated pyridine nitrogen, in low-rank coal. Some researchers found that under mild pyrolysis conditions, the relative amounts of quaternary nitrogen in the chars were lower than those in raw coals. At the same time, the relative amounts of pyridine nitrogen increased [10, 17, 19]. This change can be explained by the fact that when quaternary nitrogen exists in the protonated pyridine form, the protonated form will break up, with the loss of hydroxyl oxygen during pyrolysis [10]. Consequently, the relative amount of quaternary nitrogen decreases and that of pyridine nitrogen increases correspondingly. The significant differences in quaternary nitrogen amount between the studied oil shale samples during pyrolysis give evidence of their natural specificities. It is certain that the quaternary nitrogen in HD, MM and YJ oil shales exists in the form which is different from that in protonated pyridines, in which it is more likely to be present as pyridine structures associated with oxygen.

When the pyrolysis temperature increases to 300 °C, the relative amounts of pyridine, pyridone, quaternary nitrogen and pyridine N-oxide slightly increase, as shown in Figure 4. This is due to the release of some amount of nitrogen from raw oil shale samples in this process (see Table 2). Moreover, the loss of nitrogen is attributed to the release of chemisorbed oxygen associated nitrogen and amino nitrogen, whereas the amounts of other nitrogen functionalities remain almost constant. Therefore, the relative amounts of these nitrogen functionalities increase slightly. It should be pointed out that the N-X1 functionality is more likely to be in the form of pyridine N-oxide. This is due to that the XPS N 1s peak of pyridine N-oxide in the model compounds appears at about 403 eV [10, 19, 23]. When the pyrolysis temperature increases from 300 to 500 °C, the relative amounts of pyridine, pyridone and quaternary nitrogen functionalities continue to increase, whereas that of N-X1 functionality begins to decrease significantly. This can be explained by the transformation of N-X1 into other nitrogen functionalities. The transformation can be described as follows: pyridine N-oxide is converted into pyridone and, simultaneously, the latter is converted into pyridine and pyridine structures associated with oxygen, i.e. quaternary nitrogen. Due to similar binding energies, pyridone nitrogen (400.6 eV) and pyrrolic nitrogen (400.2 eV) cannot be distinguished by XPS. Therefore, the relative amount of pyridine N-oxide shows a significant decrease, whereas those of pyridine, pyridone and quaternary nitrogen increase. This is in agreement with the results obtained by Liu et al. [13], who found that pyridine N-oxide was transformed into pyridone nitrogen functionalities (including pyrrolic and pyridone) during Tongchuan coal pyrolysis under mild conditions (500 °C). Pels et al. [19] established that pyridone was converted into pyridine upon DE53 lignite pyrolysis under mild conditions (500 °C).

As the pyrolysis temperature increases to 600 °C, the relative amount of pyridine N-oxide continues to decrease. The relative amounts of pyridine and quaternary nitrogen functionalities in HD and MM oil shale semi-cokes

increase further, whereas that of pyridone functionality decreases. Pyridone and quaternary nitrogen functionalities become the predominant forms in the oil shale semi-cokes at 600 °C. The decrease in the relative amounts of pyridone functionality cannot be interpreted as a partial conversion of pyrrolic into pyridine, because carbazole (N-5) remains unaffected after pyrolysis at 600 °C for 1 h [19]. Therefore, it can be stated that most of the pyridone is converted into pyridine and pyridine structures associated with oxygen. The transformation of pyridone into pyridine form was also found to take place in the pyrolysis of Markham Main vitrinite at 600 °C [32]. Moreover, the relative amount of quaternary nitrogen functionality in YJ oil shale semi-coke at 600 °C shows a more obvious increase than those of the other functionalities, mostly at the expense of pyridine. The relative amount of pyridone functionality also increases. Pels et al. [19] reported that under severe pyrolysis conditions, condensation reactions of the coal matrix took place and nitrogen atoms were incorporated in the so formed graphene layers, substituting carbon atoms. The nitrogen atom at the edge of the graphene layers is identical to that of pyridine nitrogen and the one present in the interior of these layers can be seen as the atom of quaternary nitrogen. Both quaternary nitrogen and pyridine have a 6-membered ring structure. Hence, there is no C–C bond that needs to be broken down during condensation reaction. Based on the above facts, the condensation reaction of pyridine to quaternary nitrogen is likely to occur under the present conditions of pyrolysis at a temperature of 600 °C. The products of these condensation reactions are regarded as precursors of the graphene layers. So, the relative amount of quaternary nitrogen functionality increases and that of pyridine functionality decreases. The increase in the relative amount of pyridone functionality may be attributed to the reduction of pyridine N-1 oxide. The difference in nitrogen functionality distribution between the semi-cokes obtained at 600 °C is much smaller than that between raw oil shale samples, particularly HD and MM. This can be interpreted as the transformation of nitrogen functionalities into the forms that have higher thermal stabilities during pyrolysis. In the semi-cokes obtained at 600 °C, the relative amounts of pyridine, pyridone and quaternary nitrogen are still high. Hence, it can be inferred that nitrogen atoms associated with 6-membered ring structures have a high thermal stability.

4. Conclusions

1. During pyrolysis ($T \leq 600$ °C), most of the nitrogen present in raw Chinese Huadian, Maoming and Yaojie oil shale samples were retained in their semi-cokes obtained at 600 °C. The main temperature region of nitrogen removal was 400–500 °C, and the rate of release of nitrogen atoms was lower than that of carbon atoms in this region.

2. Five N 1s peaks appeared in the XPS spectra of raw oil shale samples and their semi-cokes: N-6, N-A, N-5, N-Q and N-X1. To obtain an acceptable fit, an additional peak at 404 (± 0.5) eV (N-X2) was required in the N 1s spectra of raw oil shale samples. In the spectra, N-6 and N-A represented the pyridine form and the amino form, respectively. Being the most abundant nitrogen form in most cases, N-5 could represent either pyridone or a mixture of pyridone and pyrrolic forms. N-Q was more likely to represent pyridine structures associated with oxygen, except for the YJ oil shale semi-coke obtained at 600 °C. N-X1 was possibly due to pyridine N-oxide. N-X2 represented the form that arose from oxygen chemisorbed onto nitrogen.
3. At a relatively low temperature (300 °C), the desorption reaction occurred and the amount of chemisorbed oxygen associated nitrogen decreased significantly. When the pyrolysis temperature increased gradually, mainly amino nitrogen was released. The proportion of aliphatic amino in the Huadian oil shale sample was higher than that in Maoming and Yaojie oil shale samples.
4. As the pyrolysis temperature increased from 300 to 500 °C, pyridine N-oxide was converted to pyridone and, simultaneously, pyridone was converted to pyridine and pyridine structures associated with oxygen.
5. In the semi-cokes of Huadian and Maoming oil shale samples obtained at 600 °C, most of the pyridone was converted into pyridine and pyridine structures associated with oxygen. In particular, the condensation reaction of pyridine to quaternary nitrogen occurred in the semi-coke of Yaojie oil shale sample at 600 °C, quaternary nitrogen representing here the nitrogen atoms in the interior of precursors of the graphene layers. It was found that nitrogen atoms associated with 6-membered ring structures had a high thermal stability.

Acknowledgements

This study was supported by the National Natural Scientific Foundation of China (51276034), and within the Program for Changjiang Scholars and Innovative Research Team in University, China (IRT13052).

REFERENCES

1. Qian, J. L., Wang, J. Q., Li, S. Y. World's oil shale available retorting technologies and the forecast of shale oil production. In: *Proceedings of the 18th International Offshore and Polar Engineering Conference*, Vancouver, British Columbia, Canada, July 6–11, 2008, **I**, 19–20.
2. Bunker, J. W., Crawford, P. M., Johnson, H. R. Hussert revisited – 5: Is oil shale America's answer to peak-oil challenge. *Oil Gas. J.*, 2004, **102**(30), 16–24.

3. Barkia, H., Belkbir, L., Jayaweera, S. A. A. Thermal analysis studies of oil shale residual carbon. *J. Therm. Anal. Calorim.*, 2004, **76**(2), 615–622.
4. Sklarew, D. S., Hayes, D. J. Trace nitrogen-containing species in the offgas from two oil shale retorting processes. *Environ. Sci. Technol.*, 1984, **18**(8), 600–603.
5. Mushrush, G. W., Beal, E. J., Hardy, D. R., Hughes, J. M. Nitrogen compound distribution in middle distillate fuels derived from petroleum, oil shale, and tar sand sources. *Fuel Process. Technol.*, 1999, **61**(3), 197–210.
6. Jiang, X. M., Yang, L. J., Yan, C., Hang, X. X., Yang, H. L. Experimental investigation of SO₂ and NO_x emissions from Huadian oil shale during circulating fluidized-bed combustion. *Oil Shale*, 2004, **21**(3), 249–257.
7. Akash, B. A., Jaber, J. O. Characterization of shale oil as compared to crude oil and some refined petroleum products. *Energ. Source.*, 2003, **25**(12), 1171–1182.
8. Bai, J. R., Xu, W., Pan, S., Zhang, B. X. Oil shale retorting process characteristic orthogonal carbon analysis. *J. Northeast Dianli Univ.*, 2015, **35**(5), 46–50 (in Chinese).
9. Pels, J. R., Wójtowicz, M. A., Moulijn, J. A. Rank dependence of N₂O emission in fluidized-bed combustion of coal. *Fuel*, 1993, **72**(3), 373–379.
10. Kelemen, S. R., Gorbaty, M. L., Kwiatek, P. J. Quantification of nitrogen forms in Argonne premium coals. *Energ. Fuel.*, 1994, **8**(4), 896–906.
11. Kelemen, S. R., Afeworki, M., Gorbaty, M. L., Kwiatek, P. J., Solum, M. S., Hu, J. Z., Pugmire, R. J. XPS and ¹⁵N NMR study of nitrogen forms in carbonaceous solids. *Energ. Fuel.*, 2002, **16**(6), 1507–1515.
12. Kelemen, S. R., Freund, H., Gorbaty, M. L., Kwiatek, P. J. Thermal chemistry of nitrogen in kerogen and low-rank coal. *Energ. Fuel.*, 1999, **13**(2), 529–538.
13. Liu, Y. H., Che, D. F., Li, Y. T., Hui, S. E., Xu, T. M. X-ray photoelectron spectroscopy determination of the forms of nitrogen in Tongchuan coal and its chars. *J. Xi'an Jiaotong Univ.*, 2001, **35**(7), 661–665 (in Chinese).
14. Mullins, O. C., Mitra-Kirtley, S., Van Elp, J., Cramer, S. P. Molecular structure of nitrogen in coal from XANES spectroscopy. *Appl. Spectrosc.*, 1993, **47**(8), 1268–1275.
15. Mitra-Kirtley, S., Mullins, O. C., van Elp, J., George, S. J., Chen, J., Cramer, S. P. Determination of the nitrogen chemical structures in petroleum asphaltene using XANES spectroscopy. *J. Am. Chem. Soc.*, 1993, **115**(1), 252–258.
16. Mitra-Kirtley, S., Mullins, O. C., van Elp, J., Cramer, S. P. Nitrogen chemical structure in petroleum asphaltene and coal by X-ray absorption spectroscopy. *Fuel*, 1993, **72**(1), 133–135.
17. Kelemen, S. R., Gorbaty, M. L., Kwiatek, P. J., Fletcher, T. H., Watt, M., Solum, M. S., Pugmire, R. J. Nitrogen transformations in coal during pyrolysis. *Energ. Fuel.*, 1998, **12**(1), 159–173.
18. Stańczyk, K., Dziembaj, R., Piwowska, Z., Witkowski, S. Transformation of nitrogen structures in carbonization of model compounds determined by XPS. *Carbon*, 1995, **33**(10), 1383–1392.
19. Pels, J. R., Kapteijn, F., Moulijn, J. A., Zhu, Q., Thomas, K. M. Evolution of nitrogen functionalities in carbonaceous materials during pyrolysis. *Carbon*, 1995, **33**(11), 1641–1653.

20. Wang, Q., Xu, X. C., Chi, M. S., Zhang, H. X., Cui, D., Bai, J. R. FT-IR study on composition of oil shale kerogen and its pyrolysis oil generation characteristics. *J. Fuel Chem. Technol.*, 2015, **43**(10), 1158–1166 (in Chinese).
21. Heistand, R. N. The Fischer Assay: Standard for the oil shale industry. *Energ. Source.*, 1976, **2**(4), 397–405.
22. Kelemen, S. R., Afeworki, M., Gorbaty, M. L., Sansone, M., Kwiatek, P. J., Walters, C. C., Freund, H., Siskin, M., Bence, A. E., Curry, D. J., Solum, M., Pugmire, R. J., Vandenbroucke, M., Leblond, M., Behar, F. Direct characterization of kerogen by X-ray and solid-state ^{13}C nuclear magnetic resonance methods. *Energ. Fuel.*, 2007, **21**(3), 1548–1561.
23. Pietrzak, R., Wachowska, H. The influence of oxidation with HNO_3 on the surface composition of high-sulphur coals: XPS study. *Fuel Process. Technol.*, 2006, **87**(11), 1021–1029.
24. Buckley, A. N. Nitrogen functionality in coals and coal-tar pitch determined by X-ray photoelectron spectroscopy. *Fuel Process. Technol.*, 1994, **38**(3), 165–179.
25. Liao, H. Q., Li, B. Q., Zhang, B. J. Desulfurization and denitrogenation in copyrolysis of coal with hydrogen-rich gases. *J. Fuel Chem. Technol.*, 1999, **27**(3), 268–272 (in Chinese).
26. Wang, Q., Sun, B. Z., Hu, A. J., Bai, J. R., Li, S. H. Pyrolysis characteristics of Huadian oil shales. *Oil Shale*, 2007, **24**(2), 147–157.
27. Williams, P. T., Ahmad, N. Influence of process conditions on the pyrolysis of Pakistani oil shales. *Fuel*, 1999, **78**(6), 653–662.
28. Jaber, J. O., Probert, S. D. Non-isothermal thermogravimetry and decomposition kinetics of two Jordanian oil shales under different processing conditions. *Fuel Process. Technol.*, 2000, **63**(1), 57–70.
29. Qin, K. Z., Guo, S. H. The structure research of Fu Shun and Mao Ming oil shale. 4. The content and composition of minerals. *J. Fuel Chem. Technol.*, 1987, **15**(1), 1–8 (in Chinese).
30. Baughman, G. L. *Synthetic Fuels Data Handbook*, 2nd edition. Cameron Engineers Inc, Denver, USA, 1978.
31. Gong, B., Buckley, A. N., Lamb, R. N., Nelson, P. F. XPS determination of the forms of nitrogen in coal pyrolysis chars. *Surf. Interface Anal.*, 1999, **28**(1), 126–130.
32. Jones, R. B., McCourt, C. B., Swift, P. XPS studies of nitrogen and sulphur in coal. In: *Proceedings of the International Conference on Coal Science*, Düsseldorf, September 7–9, 1981. Verlag Glückauf, Essen, 1981, 657–662.

Presented by S. Li

Received April 28, 2016